Journal of the Audio Engineering Society
Vol. 63, No. 12, December 2015 (© 2015)
DOI: http://dx.doi.org/10.17743/jaes.2015.0078

Wave Field Synthesis of Moving Sources with Retarded Stationary Phase Approximation

GERGELY FIRTHA AND PETER FIALA

Budapest University of Technology and Economics

Wave Field Synthesis (WFS) of a moving sound source is of great importance in the aspect of creating dynamic sound scenes. The article presents the strict mathematical derivation of WFS driving functions for an acoustic monopole, moving in an arbitrary direction with a uniform velocity. The derivation utilizes the traditional WFS theory for linear secondary source distributions by adapting the stationary phase approximation to moving source dynamics. By obtaining a purely time domain solution, the present approach provides a more correct synthesis compared to previous solutions for the problem and overcomes the drawbacks of the authors' previous methods (e.g., their great computational complexity).

1 INTRODUCTION

Wave Field Synthesis (WFS) is a well-established Sound Field Synthesis (SFS) technique for the reproduction of an arbitrary sound field over an extended listening area, employing a densely spaced loudspeaker arrangement termed as the secondary source distribution (SSD). The SSD driving functions need to be derived so that their resultant sound field coincides with the targeted sound field. When analytical SFS methods are considered, the targeted sound field is usually a plane wave or the field induced by an acoustic point source. WFS techniques yield the driving functions for a linear SSD from the Rayleigh integral formulation of the target field. The determination of the linear driving functions is not straightforward; several techniques exist resulting in different artifacts in the reproduced field. The traditional formulation [1, 2] concentrates mainly on the synthesis of monopoles. As an alternative [3, 4] presents a unified, more general framework.

When dynamic, time varying sound-scenes are reproduced, the synthesis of moving virtual sound sources is of great importance, with emphasis on the correct reproduction of the Doppler-frequency shift. Early implementations simulate the source motion as a sequence of stationary positions [5]. The technique results in a Doppler-like frequency variation, however, the generated sound field suffers from several artifacts. A recent approach succeeded in the incorporation of moving source dynamics into WFS theory [6, 4] and eliminated the spectral artifacts of the early implementations [6]. The method provides the exact solution for a planar SSD and gives time domain linear SSD driving functions utilizing the generalized WFS formulation introduced in [3].

In a former paper of the authors [7] a spectral solution was derived for both WFS and the Spectral Division Method. The derivation makes use of the angular frequency domain description of the field of a moving monopole and provides analytical planar and linear driving functions in the temporal frequency domain. However, the necessity of a numerical temporal inverse Fourier transform makes the solution infeasible when applied to arbitrary source time histories. The present article revisits the WFS of uniformly moving virtual sound sources. By adapting the traditional WFS approximations to the field of a moving sound source, analytically correct time domain driving functions are derived. The limitations of the authors' former solution are overcome, and alongside with the approach presented in [6] the moving source WFS theory is consummated. The presented results can be regarded as a general WFS solution for both moving and stationary point sources and can be directly used in practical applications.

The structure of the article is the following. Sec. 2 introduces the basics of WFS techniques and gives an overview of the description of moving sound sources. Sec. 3 presents the new results by adapting the description given in Sec. 2 to the WFS equation yielding the time-domain WFS driving functions. The validity of the analytical results are supported by numerical simulations presented in Sec. 4.

2 THEORETICAL BACKGROUND

2.1 Theory of Wave Field Synthesis

The arrangement used throughout the paper is shown in Fig. 1. The pressure field $p(\mathbf{x}, t)$ at the receiver position $\mathbf{x} = [x, \ y, \ z]^{\mathrm{T}}$, generated by the linear, continuous, identical

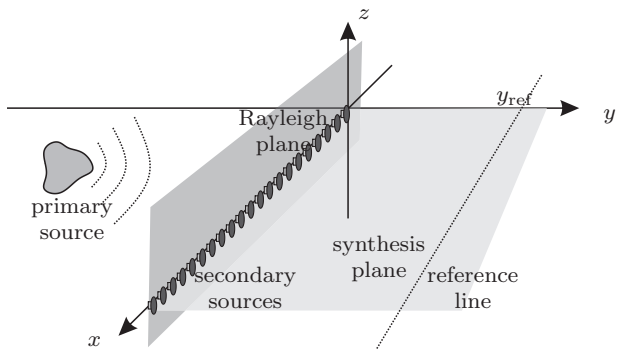

Fig. 1 WFS geometry under discussion

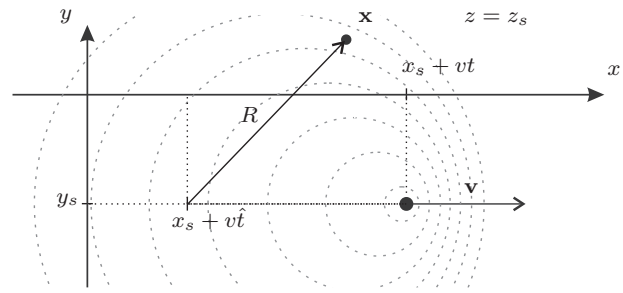

Fig. 2 Arrangement for the description of a moving sound source

point source distribution is given by

$$p(\mathbf{x}, t) = \iint_{-\infty}^{\infty} d(x_0, t_0) h(x - x_0, y, 0, t - t_0)\, \mathrm{d}x_0\, \mathrm{d}t_0, \tag{1}$$

where $h(\mathbf{x}, t)$ is the impulse response and $d(x_0, t_0)$ is the driving function of the secondary source elements.

2.1.1 Traditional 2.5D WFS

For monopole secondary sources traditional WFS solves the synthesis problem using the 3D Rayleigh integral formulation of an arbitrary sound field. In the time domain the Rayleigh integral gives the pressure field as a triple convolution:

$$p(\mathbf{x}, t) = \iiint_{-\infty}^{\infty} \overbrace{-2\, \frac{\partial}{\partial y} p(x_0, y, z_0, t_0)\Big|_{y=0}}^{d_{3\mathrm{D}}(x_0, z_0, t_0)} \times g(x - x_0, y, z - z_0, t - t_0)\, \mathrm{d}x_0\, \mathrm{d}z_0\, \mathrm{d}t_0, \tag{2}$$

where the convolution kernel is the 3D full-space Green's function $g(\mathbf{x}, t) = \frac{1}{4\pi} \delta\left(t - |\mathbf{x}|/c\right) / |\mathbf{x}|$. The Rayleigh integral provides a straightforward way of perfect synthesis by driving a planar secondary monopole distribution with the normal derivative of the desired field at $y = 0$. This technique is termed as 3D synthesis.

For linear secondary sources traditional WFS derivation utilizes the spectral formulation of the Rayleigh integral:

$$P(\mathbf{x}, \omega) = \iint_{-\infty}^{\infty} \overbrace{-2\, \frac{\partial}{\partial y} P(x_0, y, z_0, \omega)\Big|_{y=0}}^{D_{3\mathrm{D}}(x_0, z_0, \omega)} \times \frac{\mathrm{e}^{-\mathrm{j}\frac{\omega}{c}\sqrt{(x-x_0)^2 + y^2 + (z-z_0)^2}}}{\sqrt{(x - x_0)^2 + y^2 + (z - z_0)^2}}\, \mathrm{d}x_0\, \mathrm{d}z_0. \tag{3}$$

In order to obtain the driving function spectrum $D(x_0, \omega)$ for a linear secondary array, the stationary-phase method [8] can be applied. The method is based on the second order Taylor series expansion of rapidly oscillating functions, followed by an analytical integration along the z-axis and results in a frequency-dependent correction term [9, 2]. As the result of the approximation, phase-correct synthesis is restricted to the *synthesis plane*, i.e., the horizontal plane containing the virtual sound source and the SSD. Furthermore, amplitude correct synthesis is restricted to the *reference line*, parallel to the secondary sources. WFS, applying linear SSD is termed as 2.5D synthesis, referring to the fact that instead of using the 2D Green's function 3D point sources are used for the 2D synthesis problem as well.

2.1.2 Generalized 2.5D WFS

As an alternative solution it can be utilized, that reconstruction in the synthesis plane constitutes a 2D synthesis problem, for which the 2D Rayleigh integral holds. This formulation would allow perfect synthesis in the synthesis plane by a set of infinite vertical line sources at $y = 0$, driven with two times the gradient of the target field measured on $[x_0, 0, 0]^{\mathrm{T}}$. Since practical setups employ 3D SSD point sources, the 2D driving functions have to be modified in order to compensate for the secondary source dimension mismatch. This process results up again in 2.5D driving functions that can be applied directly to arbitrary target sound fields. See [3, 4] for the detailed derivation.

An important difference between the two methods lies in the application of the stationary phase approximation when a virtual point source is synthesized. Though both approaches use far-field approximations—presuming virtual sources relatively far from the SSD—traditional WFS derivation accounts for the virtual source position when applying the stationary phase approximation and references amplitude correct synthesis on the reference line. On the other hand, the correctional term of generalized 2.5D WFS is independent from the target sound field and references the synthesized field to a circle around the individual SSD elements. This results in more significant amplitude errors on the reference line. For an analysis of the amplitude deviations see [4, Ch. 5.3.2.3]. When the virtual source is sufficiently far from the SSD, the two approaches are equal [3].

2.2 Description of Moving Sources

Consider a translation invariant point source, traveling along the x-axis, located at $\mathbf{x}_s = [x_s,\ y_s,\ z_s]^{\mathrm{T}}$ at the time origin and radiating with an excitation time history $q(t)$. The arrangement is shown in Fig. 2. The radiated sound field $p_{\mathrm{m}}(\mathbf{x}, t)$ is written as the convolution of the excitation signal $q(t)$ and the time-varying impulse response g_m of the

moving load

$$p_{\mathrm{m}}(\mathbf{x}, t) = \int_{-\infty}^{\infty} g_{\mathrm{m}}(x - x_s - v\hat{t}, y - y_s, z - z_s, t - \hat{t}) q(\hat{t})\, \mathrm{d}\hat{t}, \tag{4}$$

with the impulse response of a moving monopole given by the *retarded Green's function*

$$g_{\mathrm{m}}(\mathbf{x} - \mathbf{x}_s(\hat{t}), t - \hat{t}) = \frac{1}{4\pi} \frac{\delta\left(t - \hat{t} - \frac{|\mathbf{x} - \mathbf{x}_s(\hat{t})|}{c}\right)}{|\mathbf{x} - \mathbf{x}_s(\hat{t})|}. \tag{5}$$

As given in [4, 10], expressing the distance $R(\mathbf{x}, \hat{t}) = |\mathbf{x} - \mathbf{x}_s(\hat{t})|$ of the sound source $\mathbf{x}_s$ and the receiver position $\mathbf{x}$ at the emission time instant $\hat{t}$ leads to a quadratic equation. By using the solution supposing subsonic source velocity (i.e., $v < c$), Eq. (4) can be evaluated and the radiated sound field reads

$$p_{\mathrm{m}}(\mathbf{x}, t) = \frac{1}{4\pi} \frac{q(t - \tau(\mathbf{x} - \mathbf{x}_s, t))}{\Delta(\mathbf{x} - \mathbf{x}_s, t)} \tag{6}$$

with

$$\Delta(\mathbf{x}, t) = \sqrt{(x - vt)^2 + (y^2 + z^2)(1 - M^2)}, \tag{7}$$

$$\tau(\mathbf{x}, t) = \frac{R(\mathbf{x}, t)}{c} = \frac{M(x - vt) + \Delta(\mathbf{x}, t)}{c(1 - M^2)}, \tag{8}$$

where $M = v/c$ is the *Mach number* and $\tau(\mathbf{x}, t)$ is the corresponding propagation time-delay.

The field of a virtual source moving in an arbitrary direction can be formulated by a rotation of coordinate axes. For sources moving parallel with the $z = 0$ plane and arriving to the x-axis under an angle of inclination φ, the new coordinate system $\mathbf{x}' = [x',\ y',\ z']^{\mathrm{T}}$ is defined by the transform

$$\begin{bmatrix} x' \\ y' \\ z' \end{bmatrix} = \begin{bmatrix} \cos\varphi & \sin\varphi & 0 \\ -\sin\varphi & \cos\varphi & 0 \\ 0 & 0 & 1 \end{bmatrix} \begin{bmatrix} x - x_{\mathrm{s}} \\ y - y_{\mathrm{s}} \\ z - z_s \end{bmatrix}. \tag{9}$$

In the shifted and rotated coordinate system the source is located in the origin at $\hat{t} = 0$ and travels parallel to the x'-axis, thus the radiated field is written as

$$p_{\mathrm{m}}(\mathbf{x}, t) = \frac{1}{4\pi} \frac{q(t - \tau(\mathbf{x}', t))}{\Delta(\mathbf{x}', t)}. \tag{10}$$

Note that this description of sources with arbitrary linear trajectories is equivalent with the approach proposed in [6].

3 SYNTHESIS OF MOVING SOURCES

The dynamical description given in the previous section can be directly used for 2.5D WFS of moving sources.

The recent approach introduced in [6] consists of expressing the directional gradient of the virtual sound field on the SSD and compensating the secondary source mismatch with a filter that is independent from the source position, as described in Sec. 2.1.

In the following section a new solution is presented for the application of traditional WFS theory. As the main result the stationary phase approximation of the 3D Rayleigh integral is adapted to the dynamics of a moving sound source, resulting in 2.5D WFS driving functions optimizing the synthesis on a reference line.

For convenience the derivation is given first to sources, moving parallel to the SSD, that can be easily extended for arbitrary motion trajectories with minor changes. The derivation follows the traditional stationary WFS derivation as given, e.g., in [1, 2].

3.1 Sources Moving Parallel to the SSD

Let's assume a point source moving parallel to the secondary source array, located at $\mathbf{x}_s = [x_s,\ y_s,\ 0]^{\mathrm{T}}$ at the time origin. Planar WFS driving functions are obtained by evaluating the normal derivative of the generated field Eq. (6) on the $y = 0$ plane. For the particular case of a time-harmonic excitation signal with a source frequency ω_0, the radiated field p_{m} and its directional derivative can be expressed as

$$p_{\mathrm{m}}(\mathbf{x}, t, \omega_0) = \frac{1}{4\pi} \frac{\mathrm{e}^{\mathrm{j}\omega_0(t - \tau(\mathbf{x} - \mathbf{x}_s, t))}}{\Delta(\mathbf{x} - \mathbf{x}_s, t)}, \tag{11}$$

$$\frac{\partial}{\partial y} p_{\mathrm{m}}(\mathbf{x}, t, \omega_0) = -\frac{y - y_s}{4\pi} \mathrm{e}^{\mathrm{j}\omega_0(t - \tau(\mathbf{x} - \mathbf{x}_s, t))} \times \left(\frac{(1 - M^2) + \mathrm{j}k_0 \Delta(\mathbf{x} - \mathbf{x}_s, t)}{\Delta(\mathbf{x} - \mathbf{x}_s, t)^3} \right),$$

with $k_0 = \omega_0/c$ being the source wave number. For subsonic velocities and relatively high frequencies along with large virtual source to SSD distances $|1 - M^2| < 1$ and $k_0 \Delta(\mathbf{x} - \mathbf{x}_s, t) \gg 1$, the directional derivative can be approximated as

$$\frac{\partial}{\partial y} p_{\mathrm{m}}(\mathbf{x}, t, \omega_0) \approx -\frac{\mathrm{j}k_0(y - y_s)}{4\pi} \frac{\mathrm{e}^{\mathrm{j}\omega_0(t - \tau(\mathbf{x} - \mathbf{x}_s, t))}}{\Delta(\mathbf{x} - \mathbf{x}_s, t)^2}. \tag{12}$$

Substituting Eq. (12) and the 3D Green's function into the Rayleigh integral Eq. (2) and integrating with respect to time, the following expression for the field of the moving source is obtained in the plane of synthesis ($z = 0$):

$$p(x, y, 0, t) = -\frac{\mathrm{j}k_0 y_s}{8\pi^2} \mathrm{e}^{\mathrm{j}\omega_0 t} \times \iint_{-\infty}^{\infty} \frac{\mathrm{e}^{-\mathrm{j}\omega_0\left(\frac{r}{c} + \tau(\mathbf{x}_0 - \mathbf{x}_s, t - \frac{r}{c})\right)}}{r\, \Delta(\mathbf{x}_0 - \mathbf{x}_s, t - \frac{r}{c})^2}\, \mathrm{d}x_0\, \mathrm{d}z_0, \tag{13}$$

with $\mathbf{x}_0 = [x_0,\ 0,\ z_0]^{\mathrm{T}}$ and $r = \sqrt{(x - x_0)^2 + y^2 + z_0^2}$.

In order to approximate the integral along the vertical dimension the method of stationary phase [11] is applied to Eq. (13). The approximation is given at the stationary point z^* by

$$\int_{-\infty}^{\infty} F(z) \mathrm{e}^{-\mathrm{j}\Phi(z)}\, \mathrm{d}z \approx \sqrt{\frac{2\pi}{\mathrm{j}\Phi''(z^*)}} F(z^*) \mathrm{e}^{-\mathrm{j}\Phi(z^*)}, \tag{14}$$

for an arbitrary phase function $\Phi(z)$, with Φ'' denoting its second order derivative w.r.t. z. Similar to static virtual sources, the stationary point $z^* = 0$ satisfies equation $\Phi'(z^*) = 0$. By introducing the in-plane secondary source-receiver distance $r_0 = \sqrt{(x - x_0)^2 + y^2}$, the second

derivative of the phase function will take the form (with $\mathbf{x}_0 = [x_0,\ 0,\ 0]^{\mathrm{T}}$):

$$\Phi''(0) = k_0 \left(\frac{R(\mathbf{x}_0 - \mathbf{x}_s, t - \frac{r_0}{c}) + r_0}{\Delta(\mathbf{x}_0 - \mathbf{x}_s, t - \frac{r_0}{c}) r_0} \right). \tag{15}$$

The approximation holds for rapidly oscillating exponents, i.e., $\omega_0 \left| (\frac{r}{c} + \tau(\mathbf{x}_0 - \mathbf{x}_s, t - \frac{r}{c})) \right| \gg 1$. Similarly to the stationary case this approximation will be accurate for high frequencies, or large virtual source to SSD, or large listener to SSD distances. Applying the stationary phase method integral Eq. (13) is approximated as

$$\begin{aligned} &p(x, y, 0, t) \\ &= -\frac{1}{4\pi} \sqrt{\frac{\mathrm{j}k_0}{2\pi}} \int_{-\infty}^{\infty} \sqrt{\frac{r_0}{R(\mathbf{x}_0 - \mathbf{x}_s, t - \frac{r_0}{c}) + r_0}} \\ &\quad \times \frac{y_s \mathrm{e}^{\mathrm{j}\omega_0 (t - \frac{r_0}{c} - \tau(\mathbf{x}_0 - \mathbf{x}_s, t - \frac{r_0}{c}))}}{r_0 \Delta(\mathbf{x}_0 - \mathbf{x}_s, t - \frac{r_0}{c})^{\frac{3}{2}}} \, \mathrm{d}x_0. \end{aligned} \tag{16}$$

Note that Eq. (16) contains the time-variable with a constant temporal shift $t - r_0/c$, meaning that the integral can be rewritten in the form of a temporal convolution:

$$\begin{aligned} &p(x, y, 0, t, \omega_0) \\ &= -\sqrt{\frac{\mathrm{j}k_0}{2\pi}} \iint_{-\infty}^{\infty} \sqrt{\frac{r_0}{R(\mathbf{x}_0 - \mathbf{x}_s, t_0) + r_0}} \\ &\quad \times \frac{y_s \mathrm{e}^{\mathrm{j}\omega_0 (t_0 - \tau(\mathbf{x}_0 - \mathbf{x}_s, t_0))}}{\Delta(\mathbf{x}_0 - \mathbf{x}_s, t_0)^{\frac{3}{2}}} \frac{1}{4\pi} \frac{\delta(t - t_0 - \frac{r_0}{c})}{r_0} \, \mathrm{d}x_0 \, \mathrm{d}t_0. \end{aligned} \tag{17}$$

As integral Eq. (17) explicitly contains the time-domain Green's function, comparison with Eq. (1) yields the following driving function:

$$\begin{aligned} d(x_0, t_0, \omega_0) = &-\sqrt{\frac{\mathrm{j}k_0}{2\pi}} \sqrt{\frac{r_0}{R(x_0 - x_s, y_s, t_0) + r_0}} \\ &\times \frac{y_s \mathrm{e}^{\mathrm{j}\omega_0 (t_0 - \tau(x_0 - x_s, y_s, t_0))}}{\Delta(x_0 - x_s, y_s, t_0)^{\frac{3}{2}}}. \end{aligned} \tag{18}$$

This driving function still depends on the listener position $\mathbf{x}$ through the in-plane source receiver distance r_0. For the case of a stationary virtual source it was shown in [1, Ch. 3.1] that the greatest contribution to the synthesized field is due to the SSD element located on the vector connecting the virtual source position at the emission time $[x_s + v\hat{t},\ y_s,\ 0]^{\mathrm{T}}$ and the listener position $[x, y, 0]$. This can be proven by finding the stationary phase position for the integral formulation of the synthesized field. The SSD element with the greatest contribution is shown in Fig. 3 by x^* for the general, inclined case. By using the same assumption r_0 can be approximated as $r_0 = R(x, t) \frac{|y_{\mathrm{ref}}|}{|y_s|}$ around the point of greatest contribution in integral Eq. (16) and also in the driving function:

$$d(x_0, t_0, \omega_0) = -\sqrt{\frac{\mathrm{j}k_0}{2\pi}} \sqrt{\frac{y_{\mathrm{ref}}}{y_{\mathrm{ref}} - y_s}} \frac{y_s \mathrm{e}^{\mathrm{j}\omega_0 (t_0 - \tau(x_0 - x_s, y_s, t_0))}}{\Delta(x_0 - x_s, y_s, t_0)^{\frac{3}{2}}}. \tag{19}$$

For an arbitrary source signal with the time history $q(t)$ and with the frequency content $\hat{q}(\omega)$ the driving function

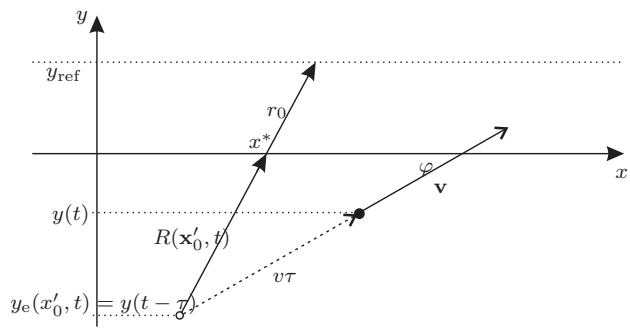

Fig. 3 Arrangement for finding $\frac{r_0}{R(\mathbf{x},t)}$ ratio. For parallel motion the y-coordinate is constant, $y(t) = y_{\mathrm{e}}(x', t) \equiv y_s$.

can be written as the weighted sum of its spectral components:

$$\begin{aligned} d(x_0, t_0) &= \int_{-\infty}^{\infty} d(x_0, t_0, \omega_0) \hat{q}(\omega_0) \, \mathrm{d}\omega_0 \\ &= \sqrt{\frac{y_{\mathrm{ref}}}{y_{\mathrm{ref}} - y_s}} \frac{-y_s}{\Delta(x_0 - x_s, y_s, t_0)^{\frac{3}{2}}} \\ &\quad \times \int_{-\infty}^{\infty} \sqrt{\frac{\mathrm{j}k_0}{2\pi}} \mathrm{e}^{\mathrm{j}\omega_0 (t_0 - \tau(x_0 - x_s, y_s, t_0))} \hat{q}(\omega_0) \, \mathrm{d}\omega_0. \end{aligned} \tag{20}$$

Eq. (20) can be recognized as the inverse Fourier transform of the excitation spectrum $\hat{q}(\omega)$, taken at $t_0 - \tau(x_0 - x_s, y_s, t_0)$, prefiltered by the transfer function $\hat{h}(\omega) = \sqrt{\frac{\mathrm{j}k}{2\pi}}$. Thus, for an arbitrary excitation the driving signals will read:

$$\begin{aligned} d(x_0, t_0) = &2\pi \sqrt{\frac{y_{\mathrm{ref}}}{y_{\mathrm{ref}} - y_s}} \frac{-y_s}{\Delta(x_0 - x_s, y_s, t_0)^{\frac{3}{2}}} \\ &\times q\,(t_0 - \tau(x_0 - x_s, y_s, t_0)) * h(t_0). \end{aligned} \tag{21}$$

3.2 Sources Moving Inclined to the SSD

The driving functions for sources moving with an angle of inclination φ towards the SSD can be easily derived in the same manner as in the parallel case. In this case the y-derivative of Eq. (10) is needed for harmonic excitation. The derivative—by neglecting the part containing the third power of $\Delta(\mathbf{x}', t)$—is given by

$$\begin{aligned} \frac{\partial}{\partial y} p_{\mathrm{m}}(\mathbf{x}, t) \approx -\frac{\mathrm{j}k_0}{4\pi} \frac{\mathrm{e}^{\mathrm{j}\omega_0 (t - \tau(\mathbf{x}', t))}}{\Delta(\mathbf{x}', t)^2} \Bigg(&\cos\varphi (y' + z') \\ &+ \sin\varphi \frac{x' - vt + M\Delta(\mathbf{x}', t)}{1 - M^2} \Bigg), \end{aligned} \tag{22}$$

where $\mathbf{x}' = [x', y', z']^{\mathrm{T}}$ is defined by Eq. (9). As the third coordinate of the coordinate system remains unchanged after the coordinate transform, the stationary phase approximation leads to the same correctional term. Following the same derivation as given in the previous subsection, the

obtained driving function reads as

$$d(x_0, t_0, \omega_0) = \sqrt{\frac{jk_0}{2\pi}}\sqrt{\frac{y_{\text{ref}}}{y_{\text{ref}} - y_e(x_0, t_0)}}\left(\cos\varphi y_0' + \sin\varphi\frac{x_0' - vt_0 + M\Delta(\mathbf{x}_0', t_0)}{1 - M^2}\right) \times \frac{e^{j\omega_0(t_0 - \tau(\mathbf{x}_0', t_0))}}{\Delta(\mathbf{x}_0', t_0)^{\frac{3}{2}}}. \quad (23)$$

While the y-coordinate of the virtual source at the time instant of emission was constant (y_s) for the parallel case, in the more general inclined case it depends both on time t_0 and the actual secondary source position x_0, and can be expressed as (see Fig. 3):

$$\begin{aligned} y_e(x_0, t_0) &= y_s + v\sin\varphi(t_0 - \tau(\mathbf{x}_0', t_0)) \quad (24)\\ &= -\left(\cos\varphi y_0' + \sin\varphi\frac{x' - vt_0 + M\Delta(\mathbf{x}_0', t_0)}{1 - M^2}\right), \end{aligned}$$

and the final result for the driving function simplifies to

$$d(x_0, t_0, \omega_0) = -\sqrt{\frac{jk_0}{2\pi}}\sqrt{\frac{y_{\text{ref}}}{y_{\text{ref}} - y_e(x_0, t_0)}}y_e(x_0, t_0) \times \frac{e^{j\omega_0(t_0 - \tau(\mathbf{x}_0', t_0))}}{\Delta(\mathbf{x}_0', t_0)^{\frac{3}{2}}}. \quad (25)$$

Note that this result takes the same form as the result for the parallel case, given by Eq. (19) with the substitution $y_s \rightarrow y_e(x_0, t_0)$.

Similarly to the parallel case the time domain driving function for an arbitrary excitation signal is given by

$$d(x_0, t_0) = -2\pi\sqrt{\frac{y_{\text{ref}}}{y_{\text{ref}} - y_e(x_0, t_0)}}y_e(x, t_0) \times \frac{q(t_0 - \tau(\mathbf{x}_0', t_0)))}{\Delta(\mathbf{x}_0', t_0)^{\frac{3}{2}}} * h(t_0). \quad (26)$$

It can be seen that the result is in perfect analogy with the traditional WFS driving function for a stationary virtual source, with the originally static distances and positions replaced by the dynamic, time-dependent equivalents. It can also be proven that substituting $v = 0$ into Eq. (23) results in the traditional stationary virtual source driving function derived in [2]. Therefore, the presented solution can be regarded as the WFS driving function, valid both for stationary and moving virtual sources. The derived driving functions are valid for non-focusing synthesis where the virtual sources are located behind the SSD.

4 NUMERICAL EXAMPLES AND COMPARISON

All simulations presented in this section were carried out by summating the fields of the monopole SSD elements in the time domain. See [4, Ch. 5.7.2.2] for a detailed explanation. In each case the reference solution was obtained by the numerical evaluation of Eq. (10).

4.1 Synthesis of a Moving Harmonic Source

The synthesis of a moving harmonic monopole with an infinite, continuous SSD is presented first. The proposed driving functions are calculated by the evaluation of Eq. (19).

The virtual source is located at $\mathbf{x}_s = [0, -1, 0]^T$ at the time origin, travels parallel to the SSD with a velocity of $v = 200$ m/s, and radiates at a frequency of $f_0 = 1$ kHz. The linear SSD is truncated at a total length of $L = 10$ m, and the spatial resolution is set to $\Delta x = 0.05$ m. The reference line is set to $y_{\text{ref}} = 1$ m. The simulation parameters were chosen aiming to exclude secondary artifacts from the investigation (spatial/temporal aliasing and truncation effects).

The snapshot of the synthesized field and the analytical reference at the time origin are depicted in Fig. 4(a) and (b). By examining the spatial distribution of the synthesized field along the reference line (Fig. 4(c)), it is revealed that—since the proposed driving functions optimize the synthesis on the reference line—the amplitude and phase of the synthesized field matches the analytical reference. This fact indicates that the suggested high-frequency assumptions are fulfilled in the presented parameter range (regarding source frequency, source-SSD distance, etc.). Slight amplitude ringing—present in the high-frequency region—are caused by the SSD truncation. By investigating the cross-section of the fields taken along the $x = 0$ line, it is confirmed that the amplitude of the synthesized and the reference fields coincide on the reference line. In other regions of the listening area, amplitude errors are present, similar to the case of a stationary virtual source investigated in details in, e.g., [12].

Figures 4(c) and (d) compare the results of the proposed approach with the recent generalized 2.5D WFS solution of [6]. The driving functions were implemented relying on [13]. Apparently, omitting the location of the source in the 2.5D correction terms results in emphasized amplitude errors in the synthesized field. The characteristics of the amplitude deviation are in accordance with the synthesis results of stationary virtual sources [4, Ch. 5.3.2.3]. This is not surprising, since the differences between the proposed and the previous 2.5D driving functions are in perfect analogy with the stationary case. Numerical simulations showed that similar to the stationary case—as it was pointed out in [3]—the presented driving functions are equal to the previous generalized driving functions as the virtual source-SSD distance tends to infinity.

In order to investigate the reproduction of the Doppler-effect the reconstructed time history is investigated next. As the investigation of secondary source truncation artifacts is out of the scope of the present paper, the SSD was lengthened to $L = 30$ m for this simulation scenario.

Fig. 5(a) presents the time history at the listening position $[0, y_{\text{ref}}, 0]^T$. It can be seen that the field synthesized using the proposed method matches the analytical reference field both in amplitude and phase with minimal error. Apart from the already discussed amplitude error, the previous generalized 2.5D WFS solution also ensures phase-correct reproduction.

The validity of the approaches is also confirmed by the investigation of the measured instantaneous frequency, captured at the same listener position, shown in Fig. 5(b). The instantaneous frequency was calculated from the phase

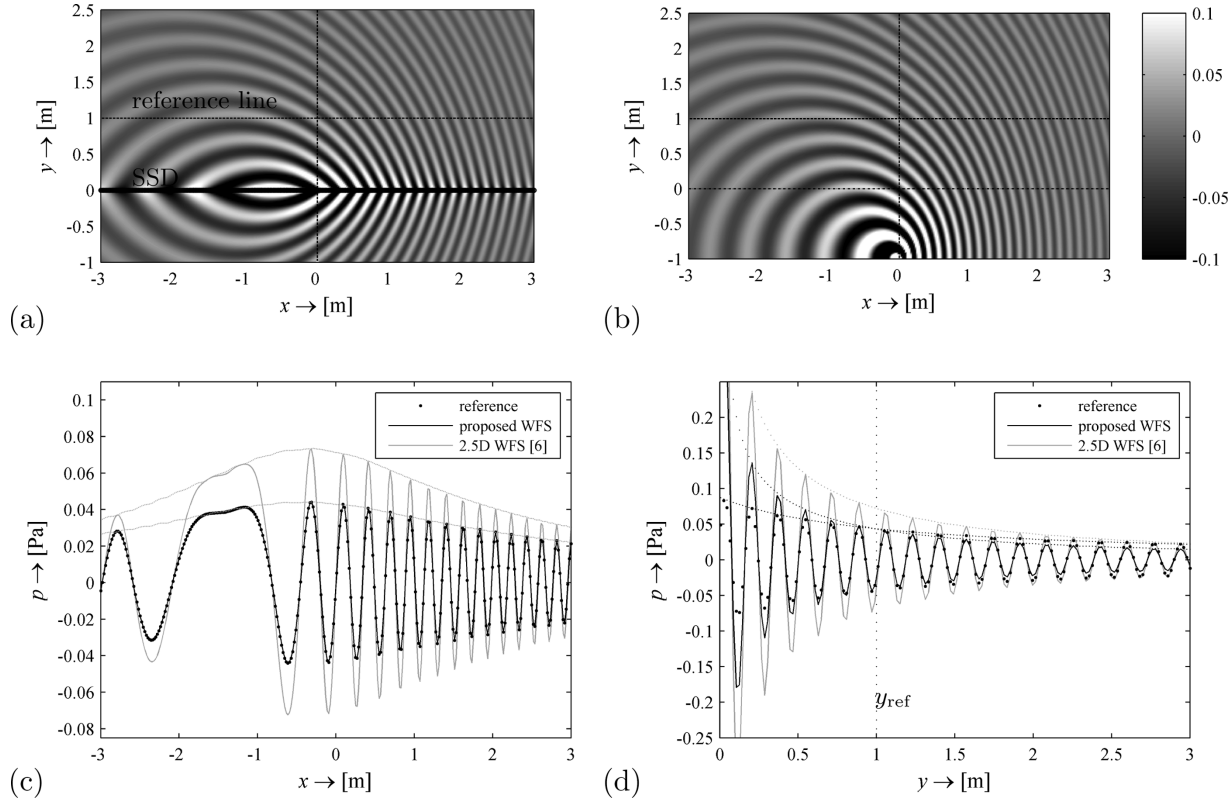

Fig. 4 Comparison of the synthesized field using WFS and the reference: Snapshots of the synthesized field using the proposed method (a) and the reference field (b) at $t = 0$. Cross-sections along the reference line ($y = y_{\mathrm{ref}}$) (c) and the y-axis ($x = 0$) (d)

difference between adjacent complex samples. This indicates that the presented WFS driving functions are capable of the correct reconstruction of the Doppler frequency-shift.

4.2 Synthesis Using Rectangular SSD Array

As the presented driving functions are valid only for sources located behind the SSD, the synthesis of a source crossing the SSD is only possible for the time regime where the virtual source is located behind the synthesis line. Furthermore, in the time interval when the virtual source is not far enough from the SSD, the synthesized field will show severe degradations, as several assumptions in the WFS approximations are no longer fulfilled (see, e.g., [12]). Due to these facts, the applicability of the presented inclined driving functions are limited, when a mere single linear SSD is considered. Even for the case of parallel source motion, a single truncated SSD restricts correct synthesis to a limited time interval.

The last simulation example presents a possible practical application of the presented driving functions: synthesis of a virtual source passing by a rectangular listening area bounded by finite linear SSDs.

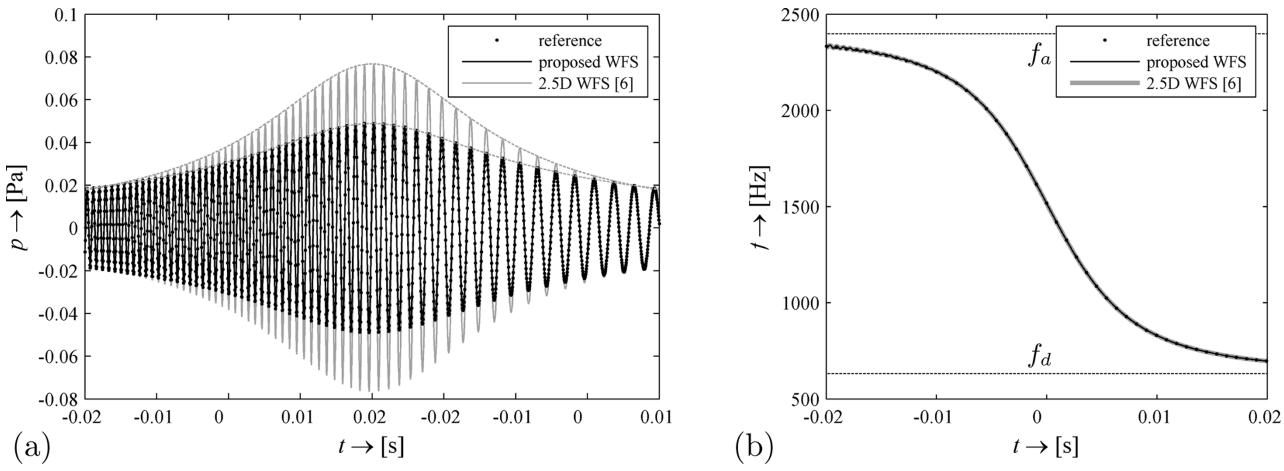

Fig. 5 Time history (a) and instantaneous frequency (b) of the SFS of a harmonic source, moving parallel to the SSD ($\varphi = 0$, $v = 200$ m/s, $f_0 = 1$ kHz). Dotted lines in (b) denote the analytical dominant Doppler-frequencies of the approaching and diverging i.e. the measured frequencies at $t = \pm\infty$, given by $\frac{f_0}{1 \pm M}$. In the present case they are $f_a \approx 2.4$ kHz and $f_d = 632$ Hz.

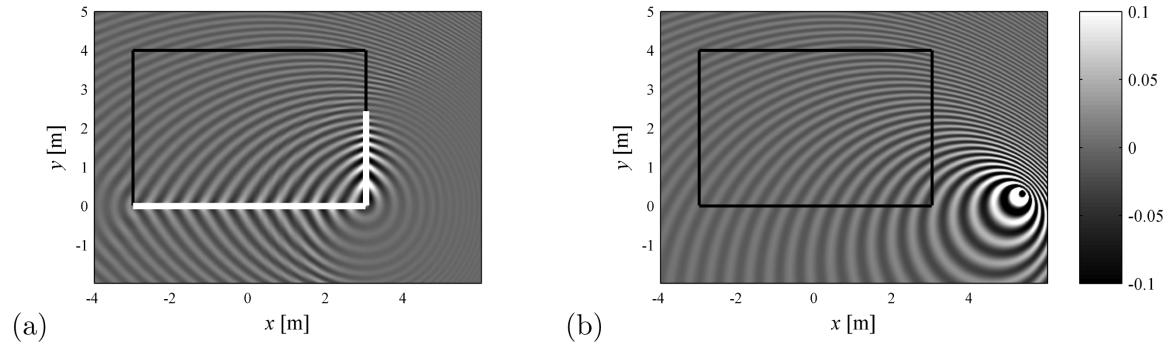

Fig. 6 Snapshot at $t = 0$ from the synthesized (a) and reference field (b) using four linear SSD elements for the SFS of a moving sound source. White line denotes the active, black line denotes the currently inactive point sources.

The simulation setup can be seen in Fig. 6. Four perpendicular linear SSD elements are used, denoted by black lines in the figure, and the synthesis area is restricted to the region bounded by the SSD ensemble. The SSD elements are $L_1 = 6$ m and $L_2 = 4$ m long with a spatial resolution of $\Delta x = 0.05$ m. The reference lines are set to $y_{\text{ref}} = 3$ m and $x_{\text{ref}} = 2$ m, respectively. Synthesis is thus optimized to the *reference point* at $\mathbf{x}_{\text{ref}} = [0,\ y_{\text{ref}},\ 0]^{\text{T}}$, located at the intersection of the two reference lines.

The simulated monopole source radiates harmonically at $f_0 = 1$ kHz. The source travels with a velocity of $v = 200$ m/s, it is positioned at $\mathbf{x}_{\text{s}} = [4,\ -1,\ 0]^{\text{T}}$ in the time origin and arrives at an angle of inclination $\varphi = 45^\circ$ to the SSD element located along the $y = 0$ line. The time history of the pass-by was sampled at 44.1 kHz.

Since the driving functions are valid only for sources behind the SSD, those SSD elements that would have to synthesize focused sources were muted. Analytically this strategy stems from the secondary source selection criterion presented in [14], extended for moving sources. In this case only those SSD elements are active where the inner product of the *instantaneous* acoustic intensity vector and the SSD element's normal vector is positive. Using this strategy in this setup each SSD element contributes to the synthesized field in different time intervals.

Snapshots of the synthesized and reference fields are presented in Fig. 6, comparing the result also with the generalized WFS approach. The figure indicates that phase correct synthesis can be achieved using the proposed driving functions; however, minor effects may be observed even in these snapshots due to the SSD elements' spatial discontinuities.

These artifacts—which are the combination of the secondary source truncation and the corner effects—are more pronounced in the time-histories, measured at the reference point, depicted in Fig. 7. As it is revealed the proposed method also suffers from a slight amplitude deviation compared to the reference, however this deviation does not exceed 1 dB. On the other hand the generalized WFS approach results in serious errors. Opposed to the proposed approach suggesting a time-dependent correction factor, generalized WFS driving functions did not consider the source motion when finding the stationary phase point, therefore the characteristics of the amplitude deviation on the reference line are time dependent resulting in enhanced artifacts.

5 CONCLUSION

The article presented time domain analytical Wave Field Synthesis driving functions for the synthesis of uniformly moving acoustic point sources revisiting the traditional WFS formulation.

The derivation adapts the traditional stationary phase approximation in the mixed temporal-frequency domain to the dynamical description of moving point sources, resulting in driving functions for harmonic sources optimized on a reference line. This formulation can be analytically

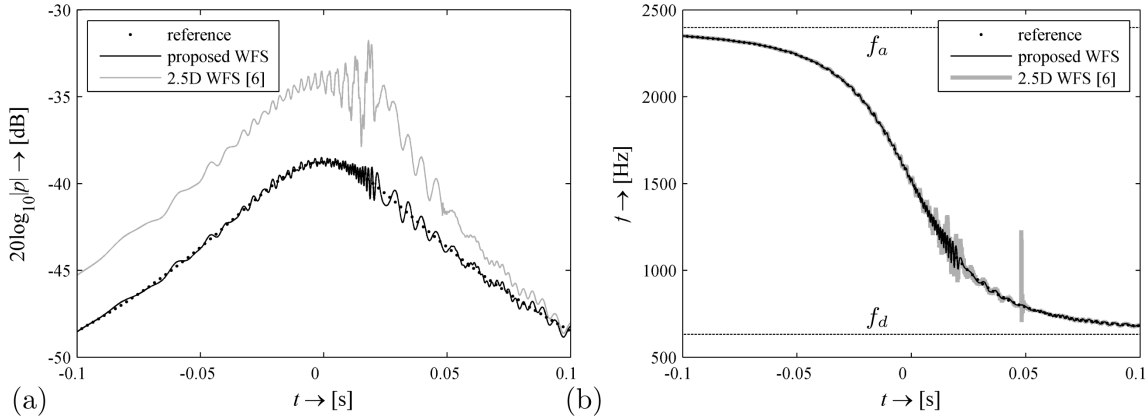

Fig. 7 Time history of the amplitude (a) and instantaneous frequency (b) at the reference point at the SFS of a moving source using multiple SSDs. Dominant frequencies are $f_a \approx 2.4$ kHz and $f_d = 632$ Hz

inverse Fourier transformed to finally obtain purely time domain driving functions for the synthesis of sources moving in arbitrary direction with an arbitrary excitation signal. The presented approach supersedes previous time domain approaches by optimizing amplitude-correct synthesis on a reference line. In this way it can be regarded as the time-domain solution of the authors' previous approach for the same problem, thus overcoming its main limitation: the great computational complexity.

As one major outcome of the article, it is proven that by applying traditional approximations the resulting driving functions formally coincide with the driving functions for stationary sources, with the originally static distances changed to dynamic distances. The validity of analytical results are demonstrated via numerical simulation examples, including a lifelike, practically applicable situation: the SFS of moving sources applying multiple linear SSD elements instead of the theoretically infinite SSD. A thorough comparison is given with the previous approaches, proving that the relation of the proposed and the previous approach is equivalent with the relation of the traditional and the generalized 2.5D WFS driving function for a stationary point source.

REFERENCES

[1] E. W. Start "*Direct Sound Enhancement by Wave Field Synthesis,"* Ph.D. thesis, Delft Univ. of Technol., Delft, The Netherlands (1997).

[2] E. Verheijen "*Sound Reproduction by Wave Field Synthesis," Ph.D. thesis*, Delft Univ. of Technol., Delft, The Netherlands (1997).

[3] S. Spors, R. Rabenstein, and J. Ahrens, "The Theory of Wave Field Synthesis Revisited," presented at the *124th Convention of the Audio Engineering Society* (2008 May), convention paper 7358.

[4] J. Ahrens, *Analytic Methods of Sound Field Synthesis*, 1st ed. (Springer, Berlin, 2012).

[5] A. Franck, A. Graefe, K. Thomas, and M. Strauss "Reproduction of Moving Sound Sources by Wave Field Synthesis: An Analysis of Artifacts," presented at the *AES 32nd Intl. Conf.: DSP For Loudspeakers* (2007 Sep.), conference paper 10.

[6] J. Ahrens and S. Spors "Reproduction of Moving Virtual Sound Sources with Special Attention to the Doppler Effect," presented at the *124th Convention of the Audio Engineering Society* (2008 May), convention paper 7363.

[7] G. Firtha and P. Fiala "Sound Field Synthesis of Uniformly Moving Virtual Monopoles," *J. Audio Eng. Soc.*, vol. 63, pp. 46–53 (2015 Jan./Feb.).

[8] E. G. Williams *Fourier Acoustics: Sound Radiation and Nearfield Acoustical Holography*, 1st ed. (Academic Press, London, 1999).

[9] A. J. Berkhout, D. de Vries, and P. Vogel "Acoustic Control by Wave Field Synthesis," *J. Acoust. Soc. Am.*, vol. 93, no. 5, pp. 2764–2778 (May 1993).

[10] P. M. Morse and K. U. Ingard *Theoretical Acoustics*, 1st ed. (McGraw-Hill Book Company, New York, NY, 1968).

[11] N. Bleistein and R. A. Handelsman *Asymptotic Expansions of Integrals* , 1st ed. (Dover Publications, 1975).

[12] S. Spors and J. Ahrens "Analysis and Improvement of Pre-Equalization in 2.5-dimensional Wave Field Synthesis," presented at the *128th Convention of the Audio Engineering Society* (2010 May), convention paper 8121.

[13] J. Ahrens Comments on simulating moving sound sources. http://www.soundfieldsynthesis.org/moving-sound-sources. Accessed: 2015-05-28.

[14] S. Spors "Extension of an Analytic Secondary Source Selection Criterion for Wave Field Synthesis," presented at the *123rd Convention of the Audio Engineering Society* (2007 Oct.), convention paper 7299.

THE AUTHORS

Gergely Firtha

Peter Fiala

Gergely Firtha was born in Budapest, Hungary, in 1986. He received his B.S. and M.S degrees from Budapest University of Technology and Economics in 2009 and 2011 respectively. Currently he is an assistant research fellow in the Laboratory of Acoutics and Studio Technics at the Department of Networked Systems and Services. His main research interests include acoustic signal processing and multichannel sound field reproduction.

•

Peter Fiala was born in Budapest, Hungary, in 1978. He received the Ph.D. degree in electrical engineering in 2009 from Budapest University of Technology and Economics. He is working as assistant professor at the Department of Networked Systems and Services. His main research interests are in the field of computational acoustics, acoustic signal processing, and noise and vibration control.